

Ocean acidification reduces net calcification and wound healing in the tropical crustose coralline alga, *Porolithon onkodes* (Corallinales, Rhodophyta)



Joshua C. Manning^{a,*}, Robert C. Carpenter^a, Elena A. Miranda^b

^a Department of Biology, California State University, Northridge, CA 91330-8303, United States of America

^b Department of Geological Sciences, California State University, Northridge, CA 91330-8266, United States of America

ARTICLE INFO

Keywords:

Carbon dioxide
Crustose coralline algae
Coral reefs
Disturbance
Ocean acidification
Porolithon onkodes

ABSTRACT

Reef dwelling algae employ a variety of physical and chemical defenses against herbivory, and the response to wounding is extremely important in algal communities. Wound healing mechanisms in crustose coralline algae (CCA) are related to skeletal growth and net calcification rate. Ocean acidification (OA) is known to affect rates of net calcification in a number of calcifying organisms, including CCA. Reduced rates of net calcification in CCA are likely to alter wound healing, and thus affect the consequences of herbivore-CCA interactions on coral reefs. The response of the tropical CCA *Porolithon onkodes* to OA and artificial wounding was quantified in a 51-day laboratory experiment. Eight artificially wounded (cut to a mean depth of 182 µm) and eight non-wounded samples of *P. onkodes* were randomly placed into each of four treatments ($n = 64$ samples total). Each treatment was maintained at a different $p\text{CO}_2$ level representative of either ambient conditions or end-of-the-century, predicted conditions (IPCC, 2014); 429.31 ± 20.84 (ambient), 636.54 ± 27.29 (RCP4.5), 827.33 ± 38.51 (RCP6.0), and 1179.39 ± 88.85 µatm (RCP8.5; mean \pm standard error). Elevated $p\text{CO}_2$ significantly reduced rates of net calcification in both wounded and non-wounded samples of *P. onkodes* (slopes = -6.4×10^{-4} and -5.5×10^{-4} $\text{mg cm}^{-2} \text{d}^{-1}$ per µatm $p\text{CO}_2$, respectively over 51 days). There also was a significant reduction in the rate of vertical regeneration of thallus tissue within the wounds as $p\text{CO}_2$ increased (slope = -1.5×10^{-3} µm d^{-1} per µatm $p\text{CO}_2$ over 51 days). This study provides evidence that elevated $p\text{CO}_2$ could reduce the ability of this important alga to recover from wounding. Because wounding by herbivores plays an important role in determining CCA community structure, we propose reduced wound healing as a mechanism by which OA might affect the structure and functional roles of CCA communities on coral reefs.

1. Introduction

Natural marine communities are subjected to a wide variety of disturbances, both physical (e.g., wave action) and biological (e.g., predation), leading to spatial and temporal heterogeneity in community structure among habitats and affecting patterns in biodiversity (Connell, 1978; Dayton, 1971; Sousa, 1984). Herbivory is a key biological disturbance affecting plant/algae communities (Dayton, 1971; Hurnly, 1991; Lubchenco, 1978), including on coral reefs (Carpenter, 1986; Lewis, 1985). Evidence from herbivore exclusion experiments (Carpenter, 1986; Lewis, 1986; Rasher et al., 2012; Smith et al., 2010; Steneck et al., 2014), and the mass mortality of the sea urchin *Diadema antillarum* in the Caribbean (Carpenter, 1985; Hughes et al., 1985;

Liddell and Ohlhorst, 1986) have highlighted the importance of herbivores in minimizing the abundance of fleshy macroalgae on coral reefs. In addition to controlling the abundance of fleshy macroalgae, herbivory also plays a role in determining the structure of crustose coralline algae communities through effects on coralline algal physiology.

Crustose coralline algae (CCA) are important members of coral reef communities, where they accrete and cement the reef framework (Adey et al., 1982; Dean et al., 2015; Littler and Doty, 1975; Nelson, 2009), and facilitate the settlement of coral larvae (Arnold et al., 2010; Harrington et al., 2004; Heyward and Negri, 1999; Price, 2010; Ritson-Williams et al., 2009). The abundance of CCA is dependent on the balance of the positive (i.e., the removal of epiphytes) and negative

Abbreviations: CCA, crustose coralline algae; IPCC, Intergovernmental Panel on Climate Change; OA, ocean acidification; PME layer, portion of the thallus including the perithallus, intercalary meristem, and epithallus; SEM, scanning electron microscope

* Corresponding author at: Department of Biological Sciences, Florida State University, 319 Stadium Drive, Tallahassee, FL 32306-4295, United States of America.

E-mail addresses: jmanning@bio.fsu.edu (J.C. Manning), robert.carpenter@csun.edu (R.C. Carpenter), elena.miranda@csun.edu (E.A. Miranda).

<https://doi.org/10.1016/j.jembe.2019.151225>

Received 4 March 2019; Received in revised form 16 August 2019; Accepted 28 August 2019
0022-0981/© 2019 Elsevier B.V. All rights reserved.

(i.e., bioerosion) effects of herbivory, and is determined by the abundance and composition of the herbivore community. Although some CCA possess antifouling defenses (i.e., shedding of epithallial cells; Johnson and Mann, 1986; Keats et al., 1997), other species rely, in part, on herbivory to remain free of epiphytes (Steneck, 1983, 1982). Because of this, the abundance of crustose coralline algae is often positively correlated with herbivore biomass (reviewed in Steneck, 1986). In general, the calcified thalli of CCA are well defended against herbivory, but multiple animal taxa, including parrotfishes and sea urchins, are able to excavate calcified tissue from CCA (Steneck, 1983, 1986). Parrotfishes vary in their importance as bioeroders, as does the frequency with which different species target CCA (Adam et al., 2015, 2018; Bellwood and Choat, 1990). Meanwhile, the importance of sea urchins as bioeroders of CCA is dependent on their abundance within the reef (O'Leary and McClanahan, 2010). In a study of CCA abundance related to grazer abundance on Kenyan coral reefs, O'Leary and McClanahan (2010) found that the cover of CCA was significantly reduced on heavily fished coral reefs where reduced predator abundance allowed sea urchins to increase in abundance. In this case, the negative effects of herbivore (i.e., sea urchin bioerosion) limited CCA abundance.

In addition to determining abundances of CCA, herbivores can have indirect effects on CCA community structure by affecting the outcome of competitive interactions. The outcome of competitive interactions among CCA are typically determined by thallus thickness, and in any given competitive bout, the CCA with the thicker thallus generally prevails (Steneck et al., 1991). Grazing by herbivores can reduce the thickness of CCA thalli, resulting in population level reversals in competitive outcomes and increased intransitivity in CCA competitive networks (Paine, 1984; Steneck et al., 1991). For example, Steneck et al. (1991) found that a thick, physically well-defended temperate CCA, *Lithophyllum impressum*, was competitively superior when herbivory was frequent and of low intensity, but was outcompeted by a thinner, fast growing CCA, *Pseudolithophyllum whidbeyense*, when herbivory was most intense. Thus, the structure of CCA communities depends on the intensity and frequency of herbivory, but also the growth strategies employed by the CCA present within each community. Generally, thick species grow more slowly and heal wounds to their thalli by regenerating tissue vertically within wounds, whereas thin species grow more rapidly and heal wounds to their thalli by growing laterally to fill them with new tissue (Steneck et al., 1991). Both growth and wound healing rely directly on rates of net calcification, a process that is being increasingly threatened by ocean acidification.

Ocean acidification (OA) is a change in ocean chemistry, namely reduced seawater pH and calcium carbonate saturation states, caused by the uptake of anthropogenic CO₂ from the atmosphere (Caldeira and Wickett, 2003; Doney et al., 2009; Hoegh-Guldberg et al., 2007; IPCC, 2014; Sabine et al., 2004). OA will likely negatively affect many calcified marine organisms, but CCA are expected to be among the first affected because they utilize a highly soluble, high-Mg calcite form of calcium carbonate (Hofmann et al., 2010; Kroeker et al., 2010, 2013; McCoy and Kamenos, 2015; Morse et al., 2006). Experimental evidence suggests that OA may reduce the recruitment, abundance, productivity, and calcification of tropical CCA (Anthony et al., 2008; Comeau et al., 2013, 2014; Diaz-Pulido et al., 2012; Jokiel et al., 2008; Kuffner et al., 2008). Additionally, OA has caused partial tissue mortality (i.e., bleaching followed by endolithic algal colonization) in CCA during experimental manipulations of seawater pCO₂ (Anthony et al., 2008; Diaz-Pulido et al., 2012). But while there is significant evidence of the negative effects of OA on CCA physiology, there has been minimal research into how these changes in physiology will affect ecological processes important to CCA success. Johnson and Carpenter (2012) found that elevated seawater pCO₂ increased the susceptibility of *Porolithon onkodes*, a common CCA throughout the Indo-Pacific, to grazing by the sea urchin *Echinothrix diadema* during an experimental manipulation, indicating the potential for interactions between OA and

natural processes like herbivory. Increased susceptibility to grazers could be the result of a weakened or thinner thallus, though this has yet to be demonstrated for this species. However, there is evidence that the cell walls and thalli of some temperate CCA are thinning as a result of OA and that changes in mineralogy and skeletal organization have made their skeletons prone to greater damage by herbivores (Burdett et al., 2012; Kamenos et al., 2013; McCoy, 2013; McCoy and Kamenos, 2018; McCoy and Ragazzola, 2014; Ragazzola et al., 2012). Reductions in net calcification due to OA also could limit the ability for CCA to heal these wounds to their thalli, but this remains an untested hypothesis.

In the present study, the effects of OA and artificial wounding, mimicking an individual grazing event, on rates of net calcification and wound healing were quantified for the CCA *Porolithon onkodes* (Heydrich) Foslie. *Porolithon onkodes* is common on coral reefs throughout the tropical Pacific Ocean and, like its congener *P. pachydermum* in the Caribbean, is conspicuous on wave-resistant algal ridges (Adey, 1975; Adey et al., 1982; Dean et al., 2015; Littler and Doty, 1975). While it plays an important role in reef cementation, *P. onkodes* does not enhance coral settlement and recruitment like other species of CCA possibly due to epithallial shedding (Harrington et al., 2004; Price, 2010). *Porolithon onkodes* is considered a thick CCA (thallus > 500 μm thick), with individual thalli becoming many centimeters thick (Adey et al., 1982; Steneck, 1986). *Porolithon onkodes* has a multilayered epithallus that protects the intercalary meristem, the cell layer that produces reproductive structures (conceptacles) and cells in the photosynthetic tissue (perithallus), from damage during grazing (Adey et al., 1982; Steneck, 1982, 1983). A multilayered epithallus may confer an advantage when dealing with wounding by herbivores. Additionally, the presence of dolomite, a magnesium-rich carbonate mineral, within the cells of *P. onkodes* may confer resistance to the effects of ocean acidification (Nash et al., 2011, 2013). This study used flow-through seawater tanks to replicate seawater chemistry of present day and future oceans with increasing pCO₂ concentrations to test the hypotheses that: (1) elevated pCO₂ would reduce rates of net calcification and wound healing in *P. onkodes*, and (2) that wounding would worsen the negative effect of elevated pCO₂ on net calcification rates.

2. Materials and methods

2.1. Sample collection and preparation

Experimental manipulations were performed at the Richard B. Gump South Pacific Research Station in Mo'orea, French Polynesia from May 24 to July 14, 2016 (51 days). Cores of *P. onkodes* were collected using an air-powered drill (McMaster-Carr) with a 3-cm diameter, diamond-tipped hole saw (McMaster-Carr). The cores were collected at a depth of ~2 m in the back reef east of Cook's Pass on the north shore (17°28'46.60"S 149°49'8.27"W) and transported to the Gump Research Station in ambient seawater. Samples were promptly placed in flowing seawater tables supplied with unfiltered seawater from Cook's Bay.

The cores were mounted to plastic bases using a marine epoxy (Coral Glue, EcoTech Marine, Allentown, PA, USA), and allowed to cure for at least 24 h in the flowing seawater tables. After the epoxy had cured, and prior to placement within experimental treatments, half of the samples were cut across their diameters (Fig. 1a) to a depth of ~300 μm using a hacksaw blade. The hacksaw blade was set into a handheld grip so that the toothed edge of the blade extended out ~300 μm from the grip edge (as measured using a digital dissecting microscope, Dino-lite Edge AM4815ZTL, Dunwell Tech, Inc., Torrance, CA). A target depth of 300 μm was chosen to mimic wounds to CCA thalli caused by parrotfishes (Steneck, 1983). Thirty-two wounded and thirty-two non-wounded samples of *P. onkodes* were randomly and evenly distributed throughout each of the four treatments (n = 8 wounded and n = 8 non-wounded samples per treatment) after a two-day acclimation period in the ambient pCO₂ treatment.

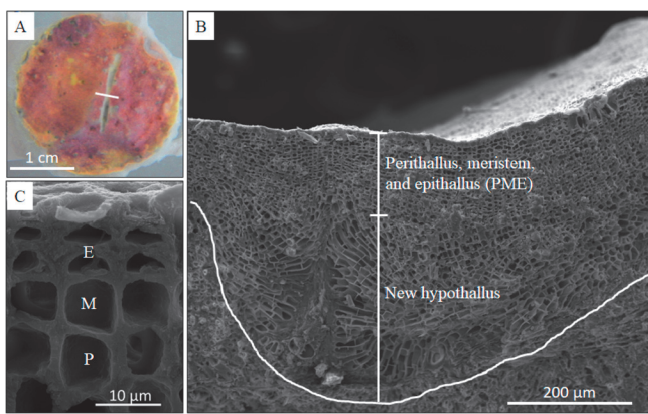


Fig. 1. (A) A wound to the thallus of *Porolithon onkodes*. A 1 cm scale bar is presented in the bottom left corner. (B) A secondary electron SEM image (346× magnification) of a cross-section through the plane of an artificial wounding (shown by white line in Fig. 1A) for *Porolithon onkodes* from the ambient $p\text{CO}_2$ treatment. The wound is outlined in white. The region of vertical growth is composed of the perithallus, intercalary meristem, and epithallus (PME layer). The new hypothallus is composed of laterally elongated cells. A 200 μm scale bar is presented in the bottom right corner. (C) A representative portion of the upper thallus of *Porolithon onkodes* (secondary electron SEM; 5000× magnification). P = perithallus, M = intercalary meristem, and E = epithallus. A 10 μm scale bar is presented at the bottom right.

2.2. Experimental design

The experiment was performed in four flow-through seawater tanks (~500 L) supplied with filtered seawater pumped from ~12 m depth in Cook's Bay and passed through a sand filter (nominal pore size ~100 μm). The seawater within each treatment was replaced continuously at a rate of ~5 L/min and flow velocity was maintained at ~0.1 m s^{-1} using water pumps (W. Lim Wave II 373 J s^{-1} ; as in Carpenter et al., 2018). Each treatment was set to one of four different $p\text{CO}_2$ levels. The ambient treatment was maintained at 429.31 ± 20.84 [mean \pm standard error (SE)] μatm $p\text{CO}_2$ using ambient seawater. The remaining three treatments were maintained at 636.54 ± 27.29 , 827.33 ± 38.51 , and 1179.39 ± 88.85 μatm (mean \pm SE), representative of predicted increases in seawater $p\text{CO}_2$ by the end of the current century under scenarios put forth by the IPCC (scenarios RCP4.5, RCP6.0, and RCP8.5 respectively; IPCC, 2014). The target

$p\text{CO}_2$ levels of the elevated treatments were achieved by bubbling pure CO_2 into each elevated treatment, while ambient air was bubbled into the ambient treatment (as in Carpenter et al., 2018). To maintain the desired pH (and $p\text{CO}_2$) setpoints within each of the elevated treatments, pH was monitored continuously by pH probes (Neptune Systems, USA) to regulate the bubbling of pure CO_2 through solenoid valves controlled by pH-stats (AquaController, Neptune Systems, USA). A nightly 0.1-unit pH reduction was used to simulate natural diurnal pH variability in the back reefs of Mo'orea (Hofmann et al., 2011).

Temperature and conductivity readings were taken daily, around mid-day, using a digital thermometer (Accuracy: $\pm 0.05^\circ\text{C}$, Digital Thermometer, Traceable Calibration Control Company, Webster, TX, USA) and a handheld pH meter (Thermo Scientific, Orion 3 STAR, Beverly, MA, USA) fitted with a pH probe calibrated with TRIS buffer (Mettler Toledo, DG115-SC; SOP 6a, Dickson et al., 2007). Temperature and conductivity measurements were used to calculate pH_T and pH-stats were adjusted as needed to maintain pH_T (and thus $p\text{CO}_2$) near target values within each of the elevated treatments. Seawater temperatures within each treatment were maintained using dedicated chillers. Each treatment was kept as close as possible to mean daily maximum sea surface temperatures measured from May to July 2011–2016 (~28.1 $^\circ\text{C}$) by a thermistor (HOBO Pro v2 Water Temperature Data Logger - U22-001, Onset Computer Corporation, Bourne, MA, USA) moored at ~1.5 m depth in the back reef near the site of sample collection (Leichter et al., 2018).

Total alkalinity (TA) and salinity of the seawater in each treatment were measured once per week, both in the day (14:00) and at night (20:00), from May 21 – July 17, 2016 (as in Carpenter et al., 2018). TA analyses were conducted in duplicate (~50 g seawater per replicate sample) for each treatment using open-cell, potentiometric titrations on an automatic titrator (Mettler Toledo, T50) following SOP 3b of Dickson et al. (2007). Salinity was measured with a conductivity meter (Thermo Scientific Orionstar A212, Waltham, MA), and analyses of certified reference material (CRM; Batch 37) provided by A.G. Dickson (Scripps Inst. of Oceanography, San Diego, CA, USA) were used to determine the accuracy and precision of TA measurements. The measurements of temperature, pH_T , TA, and salinity were then used to calculate seawater carbonate chemistry [e.g., $p\text{CO}_2$, dissolved inorganic carbon (DIC), aragonite saturation (Ω_a), calcite saturation (Ω_c), carbonate ion (CO_3^{2-}) concentration, bicarbonate ion (HCO_3^-) concentration] using the seacarb package for R statistical software (Gattuso et al., 2019). Means \pm SE are reported for temperature, salinity, pH_T , $p\text{CO}_2$, and TA (Table 1).

Table 1
Key physical and chemical parameters within experimental treatments.

Treatment	Temperature ($^\circ\text{C}$)	Salinity (psu)	pH_T	$p\text{CO}_2$ (μatm)	TA ($\mu\text{mol kg}^{-1}$)	Daily integrated PAR ($\text{mol quanta m}^{-2} \text{ day}^{-1}$)
429 μatm Overall	28.0 \pm 0.2	35.23 \pm 0.06	8.02 \pm 0.02	429.31 \pm 20.84	2297.34 \pm 5.96	10.55 \pm 0.20
Day		35.14 \pm 0.08	8.08 \pm 0.01	357.02 \pm 13.13	2282.86 \pm 7.73	
Night		35.32 \pm 0.09	7.96 \pm 0.01	501.60 \pm 19.17	2311.83 \pm 6.23	
636 μatm Overall	28.1 \pm 0.1	35.27 \pm 0.07	7.88 \pm 0.01	636.54 \pm 27.29	2299.18 \pm 5.29	9.94 \pm 0.38
Day		35.20 \pm 0.07	7.91 \pm 0.02	585.36 \pm 42.65	2286.39 \pm 6.95	
Night		35.33 \pm 0.13	7.85 \pm 0.01	687.73 \pm 26.29	2311.97 \pm 5.44	
827 μatm Overall	27.6 \pm 0.1	35.15 \pm 0.05	7.78 \pm 0.02	827.33 \pm 38.51	2292.69 \pm 8.99	10.61 \pm 0.19
Day		35.12 \pm 0.06	7.82 \pm 0.02	735.47 \pm 34.83	2279.50 \pm 12.0	
Night		35.17 \pm 0.08	7.74 \pm 0.02	919.18 \pm 54.59	2305.89 \pm 12.5	
1179 μatm Overall	28.0 \pm 0.1	35.20 \pm 0.09	7.65 \pm 0.02	1179.39 \pm 88.85	2313.16 \pm 3.71	11.40 \pm 0.45
Day		35.20 \pm 0.06	7.68 \pm 0.02	1074.44 \pm 64.04	2304.66 \pm 5.07	
Night		35.19 \pm 0.18	7.63 \pm 0.04	1284.34 \pm 163.4	2321.65 \pm 3.84	

Mean (\pm SE) of key physical and chemical parameters measured for each treatment between 21 May 2016 to 17 July 2016. Daily integrated PAR values are averaged by day (n = 51; May 24 – July 14) and account for shading. Temperature was measured daily in all treatments (n = 53; May 21 – July 14). Salinity and seawater chemistry (pH_T , $p\text{CO}_2$, and TA) were analyzed weekly (n = 9; May 21 – July 17) and overall (full day), daytime, and nighttime values presented are averages of multiple measurements made at each sampling point.

Neutral density screening was used to reduce natural sunlight reaching each treatment and simulate conditions experienced at ~ 2 m depth in the back reef (as in Carpenter et al., 2018). However, mean instantaneous PAR (range = 323.70–371.30 $\mu\text{mol m}^{-2} \text{s}^{-1}$) within the treatments was still higher than the in situ and in-lab irradiances at the onset of light saturation (I_k) reported for *P. onkodes* (205 and 124 $\mu\text{mol m}^{-2} \text{s}^{-1}$ respectively; Chisholm, 2003). Therefore, an additional piece of mesh window screening was used to further reduce light (all wavelengths) by $\sim 30\%$ to prevent excessive light oversaturation of the experimental samples. Daily integrated photosynthetically active radiation (PAR; mol quanta $\text{m}^{-2} \text{d}^{-1}$) was quantified for each treatment from measurements of PAR recorded every 30 min by an Odyssey Integrating PAR cosine sensor (Dataflow Systems Limited, Christchurch, New Zealand) placed at the center of each treatment. Sensor failure on June 4, 2016 resulted in a sudden reduction in the daily integrated PAR measurements within the ambient and RCP6.0 treatments. There was little difference in the mean instantaneous PAR for each treatment prior to this sensor failure (ambient: 342.79 ± 5.32 , RCP4.5: 374.15 ± 5.71 , RCP6.0: 348.56 ± 4.90 , RCP8.5: 326.99 ± 4.95 ; $\mu\text{mol quanta m}^{-2} \text{s}^{-1}$; data collected November 2015–June 2016). So, a correction factor, determined by taking the difference between the pooled mean instantaneous PAR for the RCP8.5 and RCP4.5 treatments and the pooled mean instantaneous PAR for the ambient and RCP6.0 treatments, was added to the instantaneous PAR values for the ambient and RCP6.0 treatments. These corrected values then were used to quantify the daily integrated PAR (mol quanta $\text{m}^{-2} \text{d}^{-1}$) for the duration of the experimental period, 24 May to 14 July 2016. The means \pm SE reported for daily integrated PAR have been corrected to account for the sensor failure and for the shading material placed over the samples (Table 1).

2.3. Net calcification and tissue mortality

Short term rates of net calcification over the course of the 51-day experiment were quantified using the buoyant weight technique (Davies, 1989). All *P. onkodes* samples were buoyant weighed in duplicate (to the nearest 1 mg; duplicate measurements ± 3 mg) prior to being placed within the ambient treatment for acclimation to treatment conditions, and again at the end of the experiment. Buoyant weights were converted to dry weights using the density of calcite (2.71 g cm^{-3}) and the difference between dry weights (final-initial) was normalized to the planar surface area of living tissue for each individual sample at day 0. These values were then divided by the total number of days in treatment (51, including a 2-day acclimation) to produce a rate of net calcification. At the end of the 51-day experiment, there was evidence of tissue mortality (i.e., tissue bleaching) in many of the samples. To quantify this loss, measurements of the planar surface area of living tissue were made by analyzing photographs taken at the beginning and end of the experiment (~ 16 MP resolution, Nikon COOLPIX AW130) in the software ImageJ (NIH). The proportion of living tissue remaining was calculated for each individual sample by dividing the total planar area of living tissue at the end of the experiment by the total planar area of living tissue at the beginning of the experiment. A proportion > 1 indicated positive lateral growth and an increase in planar surface area.

2.4. Wound healing and tissue regeneration

After the experiment, all *P. onkodes* samples were rinsed with freshwater, dried for at least 24 h at $\sim 60^\circ\text{C}$ in a drying oven, and transported back to California State University, Northridge for microscopic analysis. To quantify the rate of regeneration within the wounds of the algae, a scanning electron microscope (SEM) was used to image cross-sections of living tissue present within the wounds of the thalli of *P. onkodes* (Fig. 1). Sample preparation for SEM work included cutting, mounting, and applying a conductive coating of gold to the thalli. Cross sections of the thalli were prepared using wire cutters to cut perpendicular to, and across, the wound. These cross sections then were

mounted facing up on SEM stubs with an adhesive tab, sprayed with moisture-free air to remove any loose debris, and coated with 5 nm of gold using a sputter coater (Cressington 108auto, Watford, England) and thickness controller (Cressington MTM-20, Watford, England).

Images of the cross sections were obtained using the FEI Quanta 600 SEM at California State University, Northridge. SEM images of the wounds from each sample of *P. onkodes* with live tissue present within the wound at the end of the 51-day experiment ($n = 13$) were collected under high vacuum. Though more samples showed evidence of wound healing, the uncertainty in the time at which the tissues within their wounds died precluded them from the analysis of the rate of wound healing. Wounds were imaged at both $150\times$ and $349\times$ magnification. The SEM working conditions during imaging included an accelerating voltage of 20 kV, a beam spot size of 4, a working distance of ~ 10 mm, and filament and emission currents ranging from 1.8–2.0 A and 96–102 μA , respectively.

The wounds were identifiable by their noticeable hypothallial cell layer (Fig. 1) which forms within deeper wounds in CCA (Steneck, 1983). The hypothallus in the wounds was similar in structure to the multilayered hypothallus (important in lateral growth) present at the base and growing edge of each crust (Adey et al., 1982). The imaging software ImageJ (Schneider et al., 2012) was used to make measurements of the thickness of the regenerated tissue within the SEM images. The rate of vertical tissue regeneration was quantified by measuring the thickness of the perithallus, intercalary meristem, and epithallus (PME layer; Fig. 1), the region where vertical growth was occurring. The thickness of the PME layer was obtained by averaging the thicknesses at the deepest point within the wound, and at the midpoints (approximate) between the outer edges of the wound and the deepest point. The thickness of the PME layer then was divided by the number of days in treatment (51 including the 2-day acclimation) to create a metric for the rate of vertical regeneration. The rate of hypothallus regeneration within the wounds was quantified in a similar manner.

2.5. Statistical analysis

Means (\pm SE) are presented for temperature, salinity, pH_T , pCO_2 , TA, and daily integrated PAR (Table 1). The responses of net calcification and proportion of live tissue remaining in *P. onkodes* were analyzed with analysis of covariance (ANCOVA), using wounding treatment (wounded versus non-wounded) as the categorical independent variable and pCO_2 as the covariate. Residuals were analyzed graphically to test for the assumptions of normality and homogeneity of variance. To meet these assumptions, the data for net calcification and proportion of live tissue remaining were transformed using logit and squared transformation, respectively. Separate slope models were run for each response variable to test the effect of pCO_2 individually on wounded and non-wounded individuals of *P. onkodes*. For each response variable, models then were run to test for homogeneity of slopes, and ANCOVA was performed if it was found that the slopes were not significantly different. Coefficients for the intercepts and slopes of the individual regressions for wounded and non-wounded individuals obtained from the separate slope models were used to generate back-transformed values for the slopes and intercepts to plot on the non-transformed data. The ANCOVA analyses were performed using the `glm` command in the 'stats' package of R (version 3.2.4; R Core Team, 2016).

The rates of vertical and lateral regeneration within the wounds of *P. onkodes* were regressed on pCO_2 using a generalized linear model fit to a Gaussian (normal) distribution. Graphical analyses of residuals were used to test for the assumptions of normality and homogeneity of variances. These regression analyses also were performed using the `glm` command in the 'stats' package of R (version 3.2.4; R Core Team, 2016).

While the samples of *Porolithon onkodes* within this study were pseudoreplicated due to logistical limitations, we assumed independence of the samples for the statistical analyses. The large volume of seawater (~ 500 L) within each treatment was continuously replaced

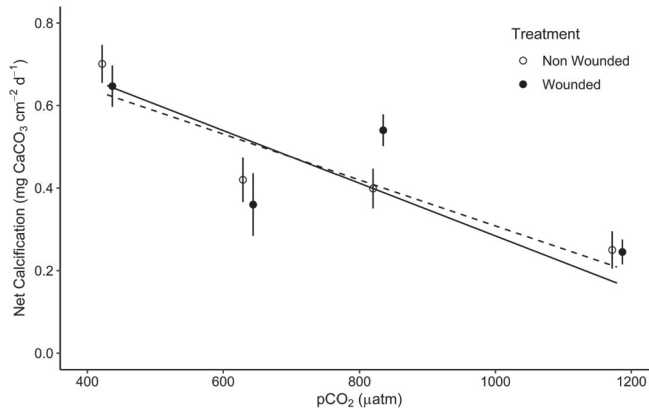


Fig. 2. Net calcification ($\text{mg CaCO}_3 \text{ cm}^{-2} \text{ d}^{-1}$) for wounded (closed circle) and non-wounded (open circle) individuals of *Porolithon onkodes* plotted against pCO_2 (μatm) as means \pm SE. The points and error bars have been offset slightly to minimize overlap. Regression lines for wounded (solid) and non-wounded (dashed) *Porolithon onkodes* were plotted from back-transformed regression coefficients. Sample sizes of the wounded (W) and non-wounded (NW) treatments for the different pCO_2 levels are as follows: 429 μatm (W = 7, NW = 8), 636 μatm (W = 8, NW = 8), 827 μatm (W = 8, NW = 8), and 1179 μatm (W = 8, NW = 8).

(flushing rate $\sim 5 \text{ L/min}$) with freshly filtered seawater. Samples were physically separated ($\sim 1\text{--}2 \text{ cm}$) during the experiment, precluding physical competition among individuals, and placement was the same within all treatments. Therefore, we would expect any community effects to be the same across all treatments. Though we acknowledge that the statistical inference presented here should be interpreted with caution, the results of this study are congruent with the results of prior studies and provide a novel mechanism by which OA might negatively affect an important reef-building coralline alga.

3. Results

3.1. Net calcification and tissue mortality

There was a significant 63% reduction in net calcification from $0.68 \pm 0.03 \text{ mg cm}^{-2} \text{ d}^{-1}$ to $0.25 \pm 0.03 \text{ mg cm}^{-2} \text{ d}^{-1}$ (mean \pm SE of pooled wounding treatments) between 429 (ambient) and 1179 μatm pCO_2 (RCP8.5), respectively (Fig. 2; $F_{1,60} = 42.106$, $p < .001$). The slopes for both wounded and non-wounded individuals of *P. onkodes* did not differ (slopes = -6.4×10^{-4} and $-5.5 \times 10^{-4} \text{ mg cm}^{-2} \text{ d}^{-1}$, respectively) and the results of the ANCOVA indicated that there was no significant difference between the two wounding treatments (intercepts = 0.92 and 0.86 respectively). Therefore, there was no effect of wounding or its interaction with elevated pCO_2 on the rates of net calcification in *P. onkodes*.

There also was a significant 55% reduction in the proportion of the planar surface area of live tissue remaining from $0.90 \pm 0.06 \text{ cm}^2$ to $0.40 \pm 0.08 \text{ cm}^2$ (mean \pm SE of pooled wounding treatments) between 429 (ambient) and 1179 μatm pCO_2 (RCP8.5), respectively (Fig. 3; $F_{1,61} = 13.423$, $p < .001$). The slopes for both wounded and non-wounded individuals (slopes = -7.3×10^{-4} and $-6.5 \times 10^{-4} \text{ cm}^2$, respectively) of *P. onkodes* were not significantly different, and the results of the ANCOVA indicated that there again was no significant difference in the responses of wounded and non-wounded individuals (intercepts = 1.14 and 1.03, respectively). Therefore, similarly to the rates of net calcification, there was no effect of wounding or its interaction with elevated pCO_2 on the proportion of live tissue remaining in *P. onkodes*.

3.2. Wound healing and tissue regeneration

The average depth of the artificial wounds at the end of the

experiment was $182 \pm 15 \mu\text{m}$ (mean \pm standard error), and the average volume of tissue removed, estimated from the average depth and average planar area of the wounds, was $2.4 \times 10^{-3} \pm 2.3 \times 10^{-4} \text{ cm}^3$ (mean \pm SE). The rate of vertical tissue regeneration, estimated from the thickness of the PME layer within wounds of *P. onkodes*, was reduced by 58% from $2.10 \pm 0.18 \mu\text{m d}^{-1}$ to $0.89 \pm 0.36 \mu\text{m d}^{-1}$ between 429 (ambient) and 1179 μatm pCO_2 (RCP8.5), respectively (means \pm SE; Fig. 4; slope = $-1.5 \times 10^{-3} \mu\text{m d}^{-1}$, $F_{1,11} = 9.701$, $p = .01$). There were no significant differences in the rates of hypothallial regeneration resulting from changes in pCO_2 ($F_{1,11} = 1 \times 10^{-4}$, $p = .993$), although there was a marginal increase at elevated pCO_2 after removing an outlying point (Fig. 5; slope = $1.1 \times 10^{-3} \mu\text{m d}^{-1}$, $F_{1,10} = 4.553$, $p = .059$).

4. Discussion

Disturbance plays an important role in determining community structure and diversity in natural communities (Connell, 1978; Dayton, 1971; Sousa, 1984). Herbivory can have an important influence on CCA communities, increasing the intransitivity of competitive networks among CCA through indirect effects on the outcome of competition (Paine, 1984; Steneck et al., 1991). Thallus thickness, regardless of herbivory, is a key determinant of the outcome of competitive interactions among corallines (Steneck et al., 1991). Therefore, net calcification and the ability to heal wounds created by herbivores (i.e., maintaining and increasing thallus thickness) are crucial to the persistence of coralline crusts.

Over the course of this 51-day experiment, rates of net calcification in *P. onkodes* were reduced 63% between ambient (429 μatm) and elevated pCO_2 (1179 μatm ; RCP8.5). Prior studies have reported reductions in net calcification and even dissolution under elevated pCO_2 for *P. onkodes* and other tropical species of CCA (Anthony et al., 2008; Comeau et al., 2013, 2014; Diaz-Pulido et al., 2012). Mean instantaneous PAR in all treatments ($> 230 \mu\text{mol m}^{-2} \text{ s}^{-1}$) was higher than the in situ and in-lab irradiances at the onset of light saturation (I_k) reported for *P. onkodes* (205 and $124 \mu\text{mol m}^{-2} \text{ s}^{-1}$ respectively; Chisholm, 2003). Increases in irradiance past I_k are unlikely to create dramatic differences in photosynthetic performance in this alga, even if light saturated photosynthesis is not achieved (Chisholm, 2003). Therefore, the reduction in the rate of net calcification presented here was unlikely to be affected by differences in irradiances among treatments.

The large reduction in net calcification in the present study could have been the result of the 55% reduction in live tissue between ambient (429 μatm) and elevated pCO_2 (1179 μatm ; RCP8.5). It is likely that reductions in live tissue among samples affected productivity and, therefore, net calcification. Two previous studies also have reported increased tissue mortality (i.e., bleaching and colonization by endolithic algae) under elevated pCO_2 in *P. onkodes* (Anthony et al., 2008; Diaz-Pulido et al., 2012). As in Diaz-Pulido et al. (2012), there was no evidence to suggest that the tissue mortality in this experiment was the result of disease (e.g., coralline lethal orange disease; Littler and Littler, 1995). Therefore, it is likely that the tissue mortality observed in this experiment was a response to the effects of OA on physiological processes. Anthony et al. (2008) suggested that bleaching of algal tissue may be the result of a disruption of photoprotective mechanisms within the algal chloroplasts as a result of reduced pH. CCA, including *Porolithon* sp., are known to possess dynamic photoinhibition strategies, including the production of dimethylsulphoniopropionate (DMSP), that may help them to tolerate high irradiances (Burdett et al., 2014). However, it is possible that oxidative stresses, due to an interaction between naturally high irradiance and elevated pCO_2 , could have played a role in the tissue mortality observed in this study. The irradiances experienced by the samples in this experiment were similar to irradiances measured at $\sim 2 \text{ m}$ depth in the back reef on the north shore of Mo'orea (Carpenter, 2016). This suggests that OA may increase

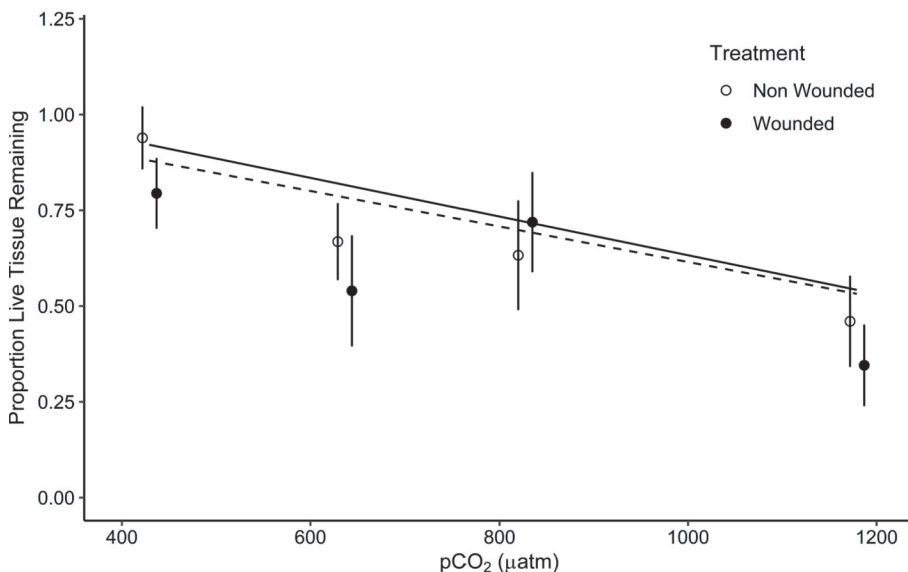


Fig. 3. Proportion live tissue remaining in wounded (closed circle) and non-wounded (open circle) individuals of *Porolithon onkodes* plotted against $p\text{CO}_2$ (μatm) as means \pm SE. The points and error bars have been offset slightly to minimize overlap. Regression lines for wounded (solid) and non-wounded (dashed) *Porolithon onkodes* were plotted from back-transformed regression coefficients. Sample sizes of the wounded (W) and non-wounded (NW) treatments for the different $p\text{CO}_2$ levels are as follows: 429 μatm (W = 7, NW = 8), 636 μatm (W = 8, NW = 8), 827 μatm (W = 8, NW = 7), and 1179 μatm (W = 8, NW = 8).

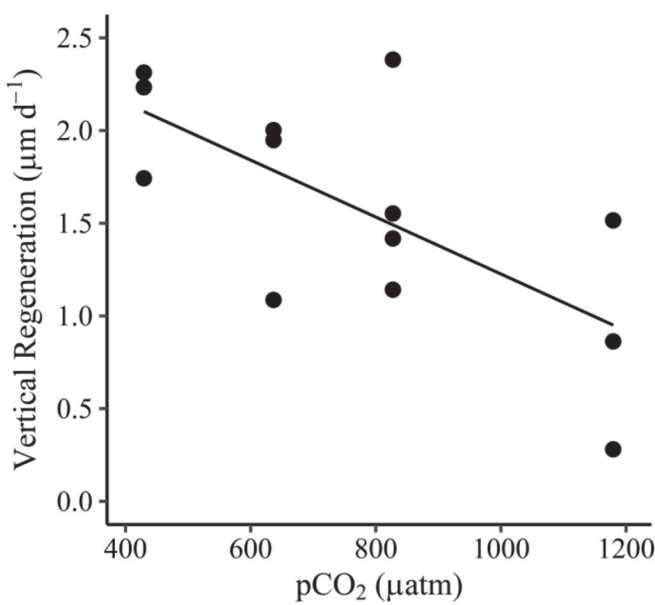


Fig. 4. The rate of vertical regeneration ($\mu\text{m d}^{-1}$) within the wounds of *Porolithon onkodes* individuals plotted against $p\text{CO}_2$ (μatm), fitted with a regression line.

photo-oxidative stresses in CCA at irradiances already experienced in the back reefs of Mo'orea, leading to bleaching and productivity loss in these important reef-builders. Future work should attempt to elucidate the mechanisms underlying bleaching in *P. onkodes* resulting from exposure to elevated $p\text{CO}_2$ and the potential for the interaction between OA and PAR on coralline physiology.

The ability to heal wounds created by herbivores is crucial to the success of corallines. Corallines have evolved mechanisms that have helped them cope with excavation by herbivores (e.g., sea urchins and parrotfish) and their abundances are often positively correlated, though not always (see O'Leary and McClanahan, 2010), with the abundance of herbivores (Steneck, 1983, 1986). We found no significant effect of artificial wounding on net calcification or tissue mortality under elevated $p\text{CO}_2$, nor was there an interactive effect of wounding and elevated $p\text{CO}_2$. *Porolithon onkodes* is considered a thick coralline, often reaching many centimeters thick, with a multilayered epithallus one to three cells thick (Adey et al., 1982; Manning personal observations). This multilayered epithallus protects the intercalary meristem, the cell

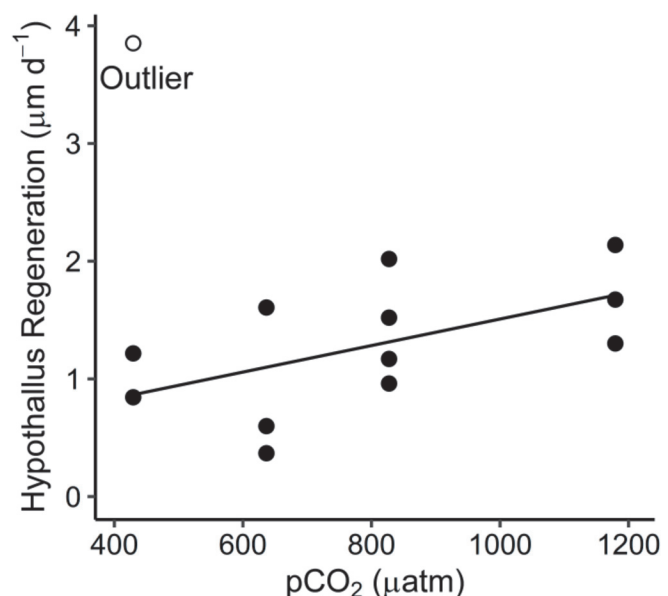


Fig. 5. The rate of regeneration of the hypothallus ($\mu\text{m d}^{-1}$) within the wounds of *Porolithon onkodes* individuals plotted against $p\text{CO}_2$ (μatm), fitted with a regression line excluding outlier (open circle).

layer that produces reproductive structures (conceptacles) and photosynthetic tissue (perithallial cells), from damage during grazing (Steneck, 1982, 1983). The multilayered epithallus and generally thick thallus of *P. onkodes* may thus confer some advantage when dealing with wounding, which could explain why wounding did not affect the net calcification and tissue mortality of *P. onkodes* in this study. This response may not be universal among crustose corallines morphologies (i.e., thick versus thin thalli) and might be mediated by the frequency of wounding (i.e., repetitive wounding). Future studies should test the effect of wounding, including repeated wounding, on the physiological responses of CCA of varying morphologies.

The present study is the first to quantify the effects of elevated $p\text{CO}_2$ on wound healing in CCA. All CCA analyzed formed a hypothallus within their wounds, as is common in deeper wounds to coralline thalli, but there was no significant effect of elevated $p\text{CO}_2$ on the rate of tissue regeneration within the hypothallus (Steneck, 1983). In contrast, there was a significant reduction in the rate of vertical tissue regeneration within wounds to the thalli of *P. onkodes* as $p\text{CO}_2$ increased, which may

be correlated with the observed reduction in net calcification. Although the wounds created in this study may not exactly match the areal extent of a parrotfish grazing wounds, the depth and volume of the wounds could be considered analogous to shallower parrotfish grazing wounds (Alwany et al., 2009; Steneck, 1983). Our results, therefore, indicate that elevated $p\text{CO}_2$ may be detrimental to the recovery of CCA from herbivore grazing. Reduced ability to heal wounds under OA could affect the relationship between CCA and their grazers, potentially leaving them increasingly susceptible to subsequent grazing (Johnson and Carpenter, 2012). However, to test this hypothesis, further experimentation is needed to determine how OA affects the ability for *P. onkodes* to recover from repeated wounding, and whether reductions in the ability to heal grazing wounds increases susceptibility to subsequent grazing. The reduction in vertical regeneration found in this study also could be a manifestation of a reduction in overall vertical growth of the thallus in *P. onkodes*. Recently, changes in competitive interactions and increased intransitivity in a competitive network of temperate CCA has been attributed to the thinning of thalli in a few thicker species of CCA (McCoy and Pfister, 2014; McCoy and Ragazzola, 2014). If the reduction in the rate of vertical tissue regeneration within wounds of *P. onkodes* found in this study is representative of a decrease in vertical growth under elevated $p\text{CO}_2$, it is possible that there could be similar shifts in competitive interaction strengths among tropical guilds of CCA. This could, in turn, have a profound effect on the functional roles of CCA on coral reefs. Therefore, additional experiments should attempt to determine whether or not the reductions in vertical tissue regeneration within wounds found here are linked to reductions in overall vertical growth of the thallus.

CCA consolidate the reef structure, and can facilitate the settlement and recruitment of coral larvae (Arnold et al., 2010; Doropoulos et al., 2012; Harrington et al., 2004; Nelson, 2009). So, understanding how changes in seawater chemistry as a result of OA affects CCA is crucial if we are to understand how OA will affect coral reef community structure and function. Few studies have explored the interaction between natural disturbances and human stressors on coral reefs (Rotjan et al., 2006; Johnson and Carpenter, 2012). The present study is the first to quantify the recovery of CCA from wounding under OA. The negative effect of elevated $p\text{CO}_2$ on the rate of wound healing in *P. onkodes* is evidence of the potential for interactive effects between natural disturbances like herbivory, and persistent stressors like OA. *Porolithon onkodes*, like its congener *Porolithon pachydermum* in the Caribbean, is among the most important CCA in structuring coral reefs and algal ridges throughout the Indo-Pacific (Adey, 1975; Adey et al., 1982; Littler and Doty, 1975; Steneck and Adey, 1976). The ability to resist and recover from grazing events is key to its functional importance. Reductions in net calcification and the ability to heal wounds could, therefore, reduce net accretion of calcium carbonate by *P. onkodes*, with implications for the future resilience of Indo-Pacific coral reefs.

Acknowledgements

The authors have no conflicts of interest to disclose. This study was supported in part by NSF grants OCE-1415268 (to Robert C. Carpenter and Peter J. Edmunds) and OCE-1236905 to the MCR LTER program. This research was completed under permits issued by the Haut-Commissariat de la République en Polynésie Française (DRRT) (Protocole d'Accueil 2015–2016). Thank you to Peter J. Edmunds, Steve Dudgeon, Sophie J. McCoy, Steeve Comeau, and Ethan C. Cissell for comments on early drafts of this manuscript. Additional thanks are given to Sarah Merolla and Bridget Shayka for assistance in sample collections. This is contribution number 293 from the CSUN Marine Biology Program.

References

Adam, T.C., Kelley, M., Ruttenberg, B.I., Burkepile, D.E., 2015. Resource partitioning along multiple niche axes drives functional diversity in parrotfishes on Caribbean coral reefs. *Oecologia* 179, 1173–1185. <https://doi.org/10.1007/s00442-015-3406-3>.

Adam, T.C., Duran, A., Fuchs, C.E., Roycroft, M.V., Rojas, M.C., Ruttenberg, B.I., Burkepile, D.E., 2018. Comparative analysis of foraging behavior and bite mechanics reveals complex functional diversity among Caribbean parrotfishes. *Mar. Ecol. Prog. Ser.* 597, 207–220. <https://doi.org/10.3354/meps12600>.

Adey, W.H., 1975. The algal ridges and coral reefs of St. Croix: their structure and Holocene development. *Atoll Res. Bull.* 187, 1–67.

Adey, W.H., Townsend, R.A., Boykins, W.T., 1982. The crustose coralline algae Rhodophyta: (Corallinaceae) of the Hawaiian islands. *Smithson. Contrib. Mar. Sci.* <https://doi.org/10.5479/si.01960768.15.1>.

Alwany, M.A., Thaler, E., Stachowitsch, M., 2009. Parrotfish bioerosion on Egyptian Red Sea reefs. *J. Exp. Mar. Biol. Ecol.* 371, 170–176. <https://doi.org/10.1016/j.jembe.2009.01.019>.

Anthony, K.R.N., Kline, D.I., Diaz-Pulido, G., Dove, S., Hoegh-Guldberg, O., 2008. Ocean acidification causes bleaching and productivity loss in coral reef builders. *Proc. Natl. Acad. Sci. U. S. A.* 105, 17442–17446. <https://doi.org/10.1073/pnas.0804478105>.

Arnold, S.N., Steneck, R.S., Mumby, P.J., 2010. Running the gauntlet: inhibitory effects of algal turfs on the processes of coral recruitment. *Mar. Ecol. Prog. Ser.* 414, 91–105. <https://doi.org/10.3354/meps08724>.

Bellwood, D.R., Choat, J.H., 1990. A functional analysis of grazing in parrotfishes (family Scaridae): the ecological implications. *Environ. Biol. Fish.* 28, 189–214.

Burdett, H.L., Aloisio, E., Calosi, P., Findlay, H.S., Widdicombe, S., Hatton, A.D., Kamemos, N.A., 2012. The effect of chronic and acute low pH on the intracellular DMSP production and epithelial cell morphology of red coralline algae. *Mar. Biol. Res.* 8, 756–763. <https://doi.org/10.1080/17451000.2012.676189>.

Burdett, H.L., Keddie, V., MacArthur, N., McDowall, L., McLeish, J., Spielvogel, E., Hatton, A.D., Kamemos, N.A., 2014. Dynamic photoinhibition exhibited by red coralline algae in the red sea. *BMC Plant Biol.* 14, 139. <https://doi.org/10.1186/1471-2229-14-139>.

Caldeira, K., Wickett, M.E., 2003. Oceanography: anthropogenic carbon and ocean pH. *Nature* 425, 365. <https://doi.org/10.1038/425365a>.

Carpenter, R.C., 1985. Sea urchin mass-mortality: effects on reef algal abundance, species composition, and metabolism and other coral reef herbivores. In: Proc. Fifth Int. Coral Reef Congr. Tahiti. vol. 4. pp. 53–60.

Carpenter, R.C., 1986. Partitioning herbivory and its effects on coral reef algal communities. *Ecol. Monogr.* 56, 345–364.

Carpenter, R.C., 2016. MCR LTER: Coral Reef: Benthic Photosynthetically Active Radiation (PAR), Ongoing since 2009. Environmental Data Initiative. <https://doi.org/10.6073/pasta/ea06e6d53df8b1cd7c1d50d025b77fd>. (Dataset accessed 8/15/2019).

Carpenter, R.C., Lantz, C.A., Shaw, E., Edmunds, P.J., 2018. Responses of coral reef community metabolism in flumes to ocean acidification. *Mar. Biol.* 165, 66. <https://doi.org/10.1007/s00227-018-3324-0>.

Chisholm, J.R.M., 2003. Primary productivity of reef-building crustose coralline algae. *Limnol. Oceanogr.* 48, 1376–1387. <https://doi.org/10.4319/lo.2003.48.4.1376>.

Comeau, S., Edmunds, P.J., Spindel, N.B., Carpenter, R.C., 2013. The responses of eight coral reef calcifiers to increasing partial pressure of CO_2 do not exhibit a tipping point. *Limnol. Oceanogr.* 58, 388–398. <https://doi.org/10.4319/lo.2013.58.1.0388>.

Comeau, S., Edmunds, P.J., Spindel, N.B., Carpenter, R.C., 2014. Fast coral reef calcifiers are more sensitive to ocean acidification in short-term laboratory incubations. *Limnol. Oceanogr.* 59, 1081–1091. <https://doi.org/10.4319/lo.2014.59.3.1081>.

Connell, J.H., 1978. Diversity in tropical rain forests and coral reefs. *Science*. <https://doi.org/10.1126/science.199.4335.1302>.

Davies, P.S., 1989. Short-term growth measurements of corals using an accurate buoyant weighing technique. *Mar. Biol.* 95, 389–395.

Dayton, P.K., 1971. Competition, disturbance, and community organization: the provision and subsequent utilization of space in a rocky intertidal community. *Ecol. Monogr.* 41, 351–389.

Dean, A.J., Steneck, R.S., Tager, D., Pandolfi, J.M., 2015. Distribution, abundance and diversity of crustose coralline algae on the Great Barrier Reef. *Coral Reefs* 34, 581–594. <https://doi.org/10.1007/s00338-015-1263-5>.

Diaz-Pulido, G., Anthony, K.R.N., Kline, D.I., Dove, S., Hoegh-Guldberg, O., 2012. Interactions between ocean acidification and warming on the mortality and dissolution of coralline algae. *J. Phycol.* 48, 32–39. <https://doi.org/10.1111/j.1529-8817.2011.01084.x>.

Dickson, A.G., Sabine, C.L., Christian, J.R., 2007. Guide to best practices for ocean CO_2 measurements. *PICES Spec. Pub.* 3, p191. <https://doi.org/10.1159/000331784>.

Doney, S.C., Fabry, V.J., Feely, R.A., Kleypas, J.A., 2009. Ocean acidification: the other CO_2 problem. *Annu. Rev. Mar. Sci.* 1, 169–192. <https://doi.org/10.1146/annurev.marine.010908.163834>.

Doropoulos, C., Ward, S., Diaz-Pulido, G., Hoegh-Guldberg, O., Mumby, P.J., 2012. Ocean acidification reduces coral recruitment by disrupting intimate larval-algal settlement interactions. *Ecol. Lett.* 15, 338–346. <https://doi.org/10.1111/j.1461-0248.2012.01743.x>.

Gattuso, J.-P., Epitalon, J.-M., Lavigne, H., Orr, J., 2019. Seacarb: Seawater Carbonate Chemistry. R package version 3.2.12. <https://CRAN.R-project.org/package=seacarb>.

Harrington, L., Fabricius, K., De'Ath, G., Negri, A., 2004. Recognition and selection of settlement substrata determine post-settlement survival in corals. *Ecology* 85, 3428–3437. <https://doi.org/10.1890/04-0298>.

Heyward, A.J., Negri, A.P., 1999. Natural inducers for coral larval metamorphosis. *Coral Reefs* 18, 273–279. <https://doi.org/10.1007/s003380050193>.

Hoegh-Guldberg, O., Mumby, P.J., Hooten, A.J., Steneck, R.S., Greenfield, P., Gomez, E., Harvell, C.D., Sale, P.F., Edwards, A.J., Caldeira, K., Knowlton, N., Eakin, C.M.,

Iglesias-Prieto, R., Muthiga, N., Bradbury, R.H., Dubi, A., Hatzios, M.E., 2007. Coral reefs under rapid climate change and ocean acidification. *Science* 318, 1737–1742. <https://doi.org/10.1126/science.1152509>.

Hofmann, G.E., Barry, J.P., Edmunds, P.J., Gates, R.D., Hutchins, D.A., Klinger, T., Sewell, M.A., 2010. The effect of ocean acidification on calcifying organisms in marine ecosystems: an organism-to-ecosystem perspective. *Annu. Rev. Ecol. Evol. Syst.* 41, 127–147. <https://doi.org/10.1146/annurev.ecolsys.110308.120227>.

Hofmann, G.E., Smith, J.E., Johnson, K.S., Send, U., Levin, L.A., Micheli, F., Paytan, A., Price, N.N., Peterson, B., Takeshita, Y., Matson, P.G., de Crook, E., Kroeker, K.J., Gambi, M.C., Rivest, E.B., Frieder, C.A., Yu, P.C., Martz, T.R., 2011. High-frequency dynamics of ocean pH: a multi-ecosystem comparison. *PLoS One* 6. <https://doi.org/10.1371/journal.pone.0028983>.

Hughes, T.P., Keller, B.D., Jackson, J.B.C., Boyle, M.J., 1985. Mass mortality of the echinoid *Diadema antillarum* Phillipi in Jamaica. *Bull. Mar. Sci.* 36, 377–384.

Huntly, N., 1991. Herbivores and the dynamics of communities and ecosystems. *Annu. Rev. Ecol. Syst.* 22, 477–503.

IPCC, 2014. In: Core Writing Team, Pachauri, R.K., Meyer, L.A. (Eds.), *Climate Change 2014: Synthesis Report. Contribution of Working Groups I, II, III to the Fifth Assessment Report of the Intergovernmental Panel on Climate Change*. IPCC, Geneva, Switzerland (151 pp).

Johnson, M.D., Carpenter, R.C., 2012. Ocean acidification and warming decrease calcification in the crustose coralline alga *Hydrolithon onkodes* and increase susceptibility to grazing. *J. Exp. Mar. Biol. Ecol.* 434–435, 94–101. <https://doi.org/10.1016/j.jembe.2012.08.005>.

Johnson, C.R., Mann, K.H., 1986. The crustose coralline alga, *Phymatolithon Foslie*, inhibits the overgrowth of seaweeds without relying on herbivores. *J. Exp. Mar. Biol. Ecol.* 96, 127–146. [https://doi.org/10.1016/0022-0981\(86\)90238-8](https://doi.org/10.1016/0022-0981(86)90238-8).

Jokiel, P.L., Rodgers, K.S., Kuffner, I.B., Andersson, A.J., Cox, E.F., Mackenzie, F.T., 2008. Ocean acidification and calcifying reef organisms: a mesocosm investigation. *Coral Reefs* 27, 473–483. <https://doi.org/10.1007/s00338-008-0380-9>.

Kamenos, N.A., Burdett, H.L., Aloisio, E., Findlay, H.S., Martin, S., Longbone, C., Dunn, J., Widdicombe, S., Calosi, P., 2013. Coralline algal structure is more sensitive to rate, rather than the magnitude, of ocean acidification. *Glob. Chang. Biol.* 19, 3621–3628. <https://doi.org/10.1111/gcb.12351>.

Keats, D.W., Knight, M.A., Pueschel, C.M., 1997. Antifouling effects of epithelial shedding in three crustose coralline algae (Rhodophyta, Corallinales) on a coral reef. *J. Exp. Mar. Biol. Ecol.* 213, 281–293. [https://doi.org/10.1016/S0022-0981\(96\)02771-2](https://doi.org/10.1016/S0022-0981(96)02771-2).

Kroeker, K.J., Kordas, R.L., Crim, R.N., Singh, G.G., 2010. Meta-analysis reveals negative yet variable effects of ocean acidification on marine organisms. *Ecol. Lett.* 13, 1419–1434. <https://doi.org/10.1111/j.1461-0248.2010.01518.x>.

Kroeker, K.J., Kordas, R.L., Crim, R.N., Hendriks, I.E., Ramajo, L., Singh, G.S., Duarte, C.M., Gattuso, J., 2013. Impacts of ocean acidification on marine organisms: quantifying sensitivities and interaction with warming. *Glob. Chang. Biol.* 19, 1884–1896. <https://doi.org/10.1111/gcb.12179>.

Kuffner, I.B., Andersson, A.J., Jokiel, P.L., Rodgers, K.S., Mackenzie, F.T., 2008. Decreased abundance of crustose coralline algae due to ocean acidification. *Nat. Geosci.* 1, 114–117. <https://doi.org/10.1038/ngeo100>.

Leichter, J., Seydel, K., Gotschalk, C., 2018. MCR LTER: Coral Reef: Benthic Water Temperature, Ongoing since 2005. knb-lter-mcr.1035.11. <https://doi.org/10.6073/pasta/1a5760c3146c574c98db854ad6d3addc>.

Lewis, S.M., 1985. Herbivory on coral reefs: algal susceptibility to herbivorous fishes. *Oecologia* 65, 370–375. <https://doi.org/10.1007/BF00378911>.

Lewis, S.M., 1986. The role of herbivorous fishes in the organization of a Caribbean reef community. *Ecol. Monogr.* 56, 183–200.

Liddell, W.D., Ohlhorst, S.L., 1986. Changes in benthic community composition following the mass mortality of *Diadema* at Jamaica. *J. Exp. Mar. Biol. Ecol.* 95, 271–278. [https://doi.org/10.1016/0022-0981\(86\)90259-5](https://doi.org/10.1016/0022-0981(86)90259-5).

Little, M.M., Doty, M.S., 1975. Ecological components structuring the seaward edges of tropical Pacific reefs: the distribution, communities and productivity of *Porolithon*. *J. Ecol.* 63, 117–129.

Little, M.M., Little, D.S., 1995. Impact of CLOD pathogen on Pacific coral reefs. *Science* 267, 1356–1360.

Lubchenco, J., 1978. Plant species diversity in a marine intertidal community: importance of herbivore food preference and algal competitive abilities. *Am. Nat.* 112, 23–39.

McCoy, S.J., 2013. Morphology of the crustose coralline alga *Pseudolithophyllum muricatum* (Corallinales, Rhodophyta) responds to 30 years of ocean acidification in the Northeast Pacific. *J. Phycol.* 49, 830–837. <https://doi.org/10.1111/jpy.12095>.

McCoy, S.J., Kamenos, N.A., 2015. Coralline algae (Rhodophyta) in a changing world: integrating ecological, physiological, and geochemical responses to global change. *J. Phycol.* 51, 6–24. <https://doi.org/10.1111/jpy.12262>.

McCoy, S.J., Kamenos, N.A., 2018. Coralline algal skeletal mineralogy affects grazer impacts. *Glob. Chang. Biol.* 24, 4775–4783. <https://doi.org/10.1111/gcb.14370>.

McCoy, S.J., Pfister, C.A., 2014. Historical comparisons reveal altered competitive interactions in a guild of crustose coralline algae. *Ecol. Lett.* 17, 475–483. <https://doi.org/10.1111/ele.12247>.

McCoy, S.J., Ragazzola, F., 2014. Skeletal trade-offs in coralline algae in response to ocean acidification. *Nat. Clim. Chang.* 1–5. <https://doi.org/10.1038/NCLIMATE2273>.

Morse, J.W., Andersson, A.J., Mackenzie, F.T., 2006. Initial responses of carbonate-rich shelf sediments to rising atmospheric pCO₂ and “ocean acidification”: role of high Mg-calcites. *Geochim. Cosmochim. Acta* 70, 5814–5830. <https://doi.org/10.1016/j.gca.2006.08.017>.

Nash, M.C., Troitzsch, U., Opdyke, B.N., Trafford, J.M., Russell, B.D., Kline, D.I., 2011. First discovery of dolomite and magnesite in living coralline algae and its geological implications. *Biogeosciences* 8, 3331–3340. <https://doi.org/10.5194/bg-8-3331-2011>.

Nash, M.C., Opdyke, B.N., Troitzsch, U., Russell, B.D., Adey, W.H., Kato, A., Diaz-Pulido, G., Brent, C., Gardner, M., Prichard, J., Kline, D.I., 2013. Dolomite-rich coralline algae in reefs resist dissolution in acidified conditions. *Nat. Clim. Chang.* 3, 268–272. <https://doi.org/10.1038/nclimate1760>.

Nelson, W.A., 2009. Calcified macroalgae—critical to coastal ecosystems and vulnerable to change: a review. *Mar. Freshw. Res.* 60, 787–801. <https://doi.org/10.1071/MF08335>.

O’Leary, J.K., McClanahan, T.R., 2010. Trophic cascades result in large-scale coralline algal loss through differential grazer effects. *Ecology* 91, 3584–3597. <https://doi.org/10.1890/09-2059.1>.

Paine, R.T., 1984. Ecological determinism in the competition for space: the Robert H. MacArthur Award Lecture. *Ecology* 65, 1339–1348.

Price, N.N., 2010. Habitat selection, facilitation, and biotic settlement cues affect distribution and performance of coral recruits in French Polynesia. *Oecologia* 163, 747–758. <https://doi.org/10.1007/s00442-010-1578-4>.

R Core Team, 2016. *R: A Language and Environment for Statistical Computing*. R Foundation for Statistical Computing, Vienna, Austria.

Ragazzola, F., Foster, L.C., Form, A., Anderson, P.S.L., Hansteen, T.H., Fietzke, J., 2012. Ocean acidification weakens the structural integrity of coralline algae. *Glob. Chang. Biol.* 18, 2804–2812. <https://doi.org/10.1111/j.1365-2486.2012.02756.x>.

Rasher, D.B., Engel, S., Bonito, V., Fraser, G.J., Montoya, J.P., Hay, M.E., 2012. Effects of herbivory, nutrients, and reef protection on algal proliferation and coral growth on a tropical reef. *Oecologia* 169, 187–198. <https://doi.org/10.1007/s00442-011-2174-y>.

Ritson-Williams, R., Arnold, S., Fogarty, N., Steneck, R.S., Vermeij, M., Paul, V.J., 2009. New perspectives on ecological mechanisms affecting coral recruitment on reefs. *Smithson. Contrib. Mar. Sci.* 437–457. <https://doi.org/10.5479/si.01960768.38.437>.

Rotjan, R.D., Dimond, J.L., Thornhill, D.J., Leichter, J.J., Helmuth, B., Kemp, D.W., Lewis, S.M., 2006. Chronic parrotfish grazing impedes coral recovery after bleaching. *Coral Reefs* 25, 361–368. <https://doi.org/10.1007/s00338-006-0120-y>.

Sabine, C.L., Feely, R.A., Gruber, N., Key, R.M., Lee, K., Bullister, J.L., Wanninkhof, R., Wong, C.S., Wallace, D.W.R., Tilbrook, B., Millero, F.J., Peng, T., Kozary, A., Ono, T., Rios, A.F., 2004. The oceanic sink for anthropogenic CO₂. *Science* 305, 367–371. <https://doi.org/10.1126/science.1097403>.

Schneider, C.A., Rasband, W.S., Eliceiri, K.W., 2012. NIH image to ImageJ: 25 years of image analysis. *Nat. Methods* 9, 671–675. <https://doi.org/10.1038/nmeth.2089>.

Smith, J.E., Hunter, C.L., Smith, C.M., 2010. The effects of top – down versus bottom – up control on benthic coral reef community structure. *Oecologia* 163, 497–507. <https://doi.org/10.1007/s00442-009-1546-z>.

Sousa, W.P., 1984. The role of disturbance in natural communities. *Annu. Rev. Ecol. Syst.* 15, 353–391.

Steneck, R.S., 1982. A limpet-coralline algal association:adaptations and defenses between a selective herbivore and its prey. *Ecology* 63, 507–522.

Steneck, R.S., 1983. Escalating herbivory and resulting adaptive trends in calcareous algal crusts. *Paleobiology* 9, 44–61. <https://doi.org/10.2307/2400629>.

Steneck, R.S., 1986. The ecology of coralline algal crusts: convergent patterns and adaptative strategies. *Annu. Rev. Ecol. Syst.* 17, 273–303. <https://doi.org/10.1146/annurev.es.17.110186.001421>.

Steneck, R.S., Adey, W.H., 1976. The role of environment in control of morphology in *Lithophyllum congestum*, a Caribbean algal ridge builder. *Bot. Mar.* 19, 197–215.

Steneck, R.S., Hacker, S.D., Dethier, M.N., 1991. Mechanisms of competitive dominance between crustose coralline algae: an herbivore-mediated competitive reversal. *Ecology* 72, 938–950. <https://doi.org/10.2307/1940595>.

Steneck, R.S., Arnold, S.N., Mumby, P.J., 2014. Experiment mimics fishing on parrotfish: insights on coral reef recovery and alternative attractors. *Mar. Ecol. Prog. Ser.* 506, 115–127. <https://doi.org/10.3354/meps10764>.